

Change in porosity is the major determinant of the variation of cortical bone elasticity at the millimeter scale in aged women

Mathilde Granke^{a,b,*}, Quentin Grimal^{a,b}, Amena Saïed^{a,b}, Pierre Nauleau^{a,b},
Françoise Peyrin^{c,d}, Pascal Laugier^{a,b}

^a UPMC Univ Paris 06, UMR 7623, Laboratoire d'Imagerie Paramétrique, 75005 Paris, France

^b CNRS, UMR 7623, Laboratoire d'Imagerie Paramétrique, 75005 Paris, France

^c CREATIS INSERM U1044, CNRS 5220, INSA Lyon, Université de Lyon, 69621 Villeurbanne Cedex, France

^d ESRF, 38043 Grenoble, France

ARTICLE INFO

Article history:

Received 20 May 2011

Revised 16 July 2011

Accepted 1 August 2011

Available online xxxx

Edited by: David Burr

Keywords:

Anisotropic elasticity

Cortical porosity

Mechanical model

Scanning acoustic microscopy

Ultrasound

ABSTRACT

At the mesoscale (i.e. over a few millimeters), cortical bone can be described as two-phase composite material consisting of pores and a dense mineralized matrix. The cortical porosity is known to influence the mesoscopic elasticity. Our objective was to determine whether the variations of porosity are sufficient to predict the variations of bone mesoscopic anisotropic elasticity or if change in bone matrix elasticity is an important factor to consider. We measured 21 cortical bone specimens prepared from the mid-diaphysis of 10 women donors (aged from 66 to 98 years). A 50-MHz scanning acoustic microscope (SAM) was used to evaluate the bone matrix elasticity (reflected in impedance values) and porosity. Porosity evaluation with SAM was validated against Synchrotron Radiation μ CT measurements. A standard contact ultrasonic method was applied to determine the mesoscopic elastic coefficients. Only matrix impedance in the direction of the bone axis correlated to mesoscale elasticity (adjusted $R^2 = [0.16-0.25]$, $p < 0.05$). The mesoscopic elasticity was found to be highly correlated to the cortical porosity (adj- $R^2 = [0.72-0.84]$, $p < 10^{-5}$). Multivariate analysis including both matrix impedance and porosity did not provide a better statistical model of mesoscopic elasticity variations. Our results indicate that, for the elderly population, the elastic properties of the mineralized matrix do not undergo large variations among different samples, as reflected in the low coefficients of variation of matrix impedance (less than 6%). This work suggests that change in the intracortical porosity accounts for most of the variations of mesoscopic elasticity, at least when the analyzed porosity range is large (3–27% in this study). The trend in the variation of mesoscale elasticity with porosity is consistent with the predictions of a micromechanical model consisting of an anisotropic matrix pervaded by cylindrical pores.

© 2011 Published by Elsevier Inc.

Introduction

Bones of different individuals not only have different sizes and shapes, but also different material properties. These characteristics entirely determine the elastic response of a bone to a given mechanical loading. The elastic properties of cortical bone tissue, which has a hierarchical organization, must be described in a multiscale framework: the structure and mechanical properties at one hierarchical level determine the properties of the subsequent one. The *mesoscale* designates the intermediate scale between the microscale (lamellar structures) and the macroscale (organ level). More precisely, the

characteristic size of a mesoscopic volume will be larger than 1.5 mm [1] and smaller than the thickness of the cortical shell. The mesoscale elastic properties are of first interest because they depend on tissue properties at all small-scale hierarchical levels and they have a direct influence on the macroscopic mechanical response of bones. The observed intra-individual [2] and inter-individual [3,4] variations of mesoscale elasticity are footprints of the remodeling process and the structure–function adaptation mechanisms of bone. This calls for a clear understanding of the variables that govern bone mesoscopic elasticity variations.

At the mesoscale, bone can be described as a two-phase composite material: a dense mineralized matrix and a soft phase, hereinafter referred to as vascular porosity [5], which consists of Haversian canals and resorption cavities containing fluids and soft tissues. The porosity has been established to be an important determinant of the bone mesoscopic elastic properties [6–8]. On the other hand, one would expect that variations of the mineralized matrix properties strongly affect the mesoscopic elasticity because the matrix occupies

* Corresponding author at: Laboratoire d'Imagerie Paramétrique, 15 rue de l'Ecole de Médecine, 75006 Paris, France. Fax: +33 1 46 33 56 73.

E-mail addresses: mathilde.granke@gmail.com (M. Granke), quentin.grimal@upmc.fr (Q. Grimal), amena.saied@upmc.fr (A. Saïed), pierre.nauleau@upmc.fr (P. Nauleau), peyrin@esrf.fr (F. Peyrin), pascal.laugier@upmc.fr (P. Laugier).

about 85% of the cortical bone volume. However, the actual influence of matrix properties variations on mesoscale elasticity is still a matter of debate in the literature. Changes in matrix mineralization have been shown to be correlated with the mesoscopic mechanical properties variations when the data were combined from eighteen species [9], but not when only human data were considered [10]. Rho et al. [7] found that the matrix elasticity (probed with nanoindentation) was significantly correlated to the mesoscopic axial Young's modulus. Since both vascular porosity and matrix properties determine mesoscale elasticity, it is not possible to draw general conclusions unless both porosity and matrix properties are measured on the same samples. To our knowledge, only Rho et al. [7] investigated to what extent the changes in porosity and matrix elasticity contribute to the variations of the mesoscopic elasticity. They found a significant correlation of both variables with the mesoscopic elasticity variations. Unfortunately, the elastic properties and the porosity were assessed on different specimens and along the bone axis direction only. Human cortical bone possesses anisotropic elastic properties which are often approximated by transversely isotropic or orthotropic properties both at the microscale [11] and mesoscale [3,12]. The preferential orientation of the pores and the mineralized fibrils are such that the relationships between matrix properties, porosity and mesoscale elasticity may be significantly different in the axial, radial and tangential directions of bone.

The objective of this work was to assess the relative contributions of vascular porosity and mineralized matrix elasticity to the mesoscopic elasticity variations in mature human cortical bone. To this purpose, experiments were designed following two requirements, which constitute the originality of the work. First, the bone matrix elasticity (reflected in acoustical impedance values) and porosity, as well as the mesoscopic elasticity, were measured on the same samples. Second, elasticity measurements at both the micro and the mesoscale were performed in three orthogonal directions. Finally, the experimental results were compared with the predictions of a micromechanical model to question the assumption that cortical bone can be modeled as a homogeneous transversally isotropic matrix pervaded by cylindrical pores.

Material and methods

Bone sample preparation

Fresh bone specimens were prepared from a collection of ten left femurs of female cadavers (mean donor age 81 years, range 66–98 years). Femurs were removed during multi-organ collection and stored at -20°C . Ethical approval for the collection of samples was granted by the Human Ethics Committee of the Centre du don des Corps at the University Paris Descartes (Paris, France). The tissue donors or their legal guardians provided informed written consent to give their tissue for investigation, in accord with legal clauses stated in the French Code of Public Health. A cross-section of thickness approximately 7 mm was cut in the mid-diaphysis of each femur. In order to maximize the variability of bone properties, parallelepiped-shaped samples were harvested from different anatomical quadrants (lateral, medial, posterior) of each cross-section. No sample was extracted in areas where the cortical thickness was less than 4 mm. This led to a set of twenty-one samples (nominally $5 \times 5 \times 7 \text{ mm}^3$): three samples from two of the femurs, two samples from seven other femurs and one sample from the remaining femur. The samples faces were oriented according to the radial (axis 1), circumferential (axis 2), and axial (axis 3) directions defined by the anatomic shape of the femoral diaphysis [2]. The samples were defatted for 12 h in a chemical bath of diethylether and methanol (1:1). The parallelism of the opposite faces was controlled with a $50 \mu\text{m}$ admitted error. The six faces of each sample were polished with a hard synthetic cloth using $3 \mu\text{m}$ polycrystalline diamond abrasive particles followed by a

$0.05 \mu\text{m}$ aluminum oxide suspension (Metadi Supreme and Masterprep, Buehler® GmbH, Düsseldorf, Germany). After preparation, the samples were stored in gauze soaked in saline solution at 4°C for no more than 48 h prior to measurements.

Assessment of mesoscale elasticity

Mesoscale elasticity was determined using a well-established method based on the measurements of ultrasonic bulk wave velocities and sample apparent mass density. The method, which has been extensively described elsewhere [2,12], is the only existing method which provides measurements of the shear and longitudinal elastic properties in the different directions of a same bone material volume. In contrast, mechanical methods (traction, torsion, three-point bending, etc.) usually require to prepare one sample for the measurement of each property. Given the ultrasonic bulk wave velocities v and apparent density ρ , the diagonal terms C_{ii} of the mesoscopic elastic tensor are calculated from:

$$\begin{aligned} C_{ii} &= \rho \cdot v_{ii}^2 \quad (i = 1, 2, 3) \\ C_{44} &= \rho \cdot v_{23}^2 = \rho \cdot v_{32}^2 \\ C_{55} &= \rho \cdot v_{13}^2 = \rho \cdot v_{31}^2 \\ C_{66} &= \rho \cdot v_{12}^2 = \rho \cdot v_{21}^2 \end{aligned} \quad (1)$$

where C_{11} , C_{22} , and C_{33} are the so called longitudinal elastic coefficients which represent the stiffness in a traction-compression mode, and C_{44} , C_{55} , C_{66} are the shear coefficients. Velocity v_{ji} denotes the velocity of a bulk wave propagating in direction i with particles motion in the j -direction. For longitudinal waves, $i=j$, and for shear waves, $i \neq j$. Samples were measured undrained in ambient conditions. The apparent mass density of each sample was assessed by dividing its mass by its volume; geometrical dimensions were measured with a digital caliper (accuracy: $\pm 0.02 \text{ mm}$) and mass with a laboratory scale (accuracy: $\pm 0.1 \text{ mg}$). The ultrasonic (US) wave velocities were evaluated using a pulse transmission method with a pair of frequency matched transducers in contact with the sample surface. Longitudinal waves and shear waves were measured using 2.25 MHz and 1 MHz transducers (respectively, V105RM and V152RM, Panametrics, Inc., Waltham, MA). Since the longitudinal and shear wave velocities in bone are significantly different ($\sim 3700 \text{ m/s}$ and 1700 m/s , respectively), the use of different frequencies for these two propagation modes allowed obtaining a similar wavelength, of the order of 1.7 mm. Hence, the resulting wavelength, which defines the probing scale, guaranteed to retrieve the bone mesoscopic elasticity (i.e. at a scale much larger than the vascular pores). The received signal was acquired using an oscilloscope (TDS 2012, Tektronix Inc., Beaverton, OR) and post-processed with a custom MatLab program (The Mathworks Inc., Natick, MA). The time delay, Δt , for wave transmission through the specimen was obtained as the difference between the arrival time of the US pulse with the sample inserted and the arrival time of a reference signal (transducers in contact for the longitudinal waves, Plexiglas plate inserted between the transducers for the shear waves). Each longitudinal coefficient was calculated after averaging the velocities measured in ten successive acquisitions with intermediate repositioning; each shear coefficient was obtained after averaging the two shear wave velocities from which it could be calculated (Eq. (1)).

The accuracy of the elastic coefficients evaluation was determined from measurements on a homogeneous calibrated pure polycrystalline (99.95%) copper plate (Goodfellow SARL, Lille, France) and was found to be 2.1% and 0.9% for the longitudinal and shear elastic coefficients, respectively. Measurement errors were assessed by repeating longitudinal and shear waves velocity measurements on two

human bone specimens for five consecutive days with intermediate repositioning. The reproducibility was 3.2% and 4.7% for the mesoscopic longitudinal and shear elastic coefficients, respectively. Finally, our measurements were verified to be bulk wave velocities and not bar wave velocities [3]. For this, longitudinal wave velocities were measured in eight artificial composite bone samples (Sawbones, Pacific Research Laboratory Inc, Vashon WA) of dimensions $10 \times 20 \times d$ mm³ (thickness \times cross-sectional dimension), the lateral dimension d varying from 2 to 10 mm. The same velocity was measured for all the Sawbone samples (2907 ± 11 m/s). The value corresponds to the tabulated bulk velocity for this material (2890 m/s). Thus, the velocities measured in this study, even for the smallest samples, were proved to be bulk wave velocities and Eq. (1) can be applied to derive the elastic coefficients.

50-MHz scanning acoustic microscopy

A custom scanning acoustic microscope (SAM), operating with a spherically focused 50-MHz transducer (V605, Valpey Fisher, Hopkinton, USA), was used to probe the acoustic impedance normal to the samples surfaces according to the measurement procedure extensively detailed in previous studies [13,14]. The acoustic impedance (Z), which is modeled as the square root of the product of the local mass density and elastic coefficient in the beam direction, has been shown to be a surrogate measurement of the bone matrix elasticity at the microscale [15]. This is also reflected by the good agreement between the impedance and the Young's modulus of bone matrix as obtained from site-matched SAM and nanoindentation measurements in bone [16,17] (although some discrepancies appear presumably due to the assumptions made on the Poisson ratio). Calibrated impedance maps were obtained with a lateral resolution of 30 μ m for all six faces of each sample. The Z-maps were segmented allowing the separation of vascular porosity and bone matrix as previously reported [18].

The acoustic impedance of the matrix was determined from the segmented maps for each face of the twenty-one samples. Note that the small pores (Volkmann's canal, osteocyte lacunae) could not be resolved so that they contributed to the probed bulk matrix properties. Matrix impedance in the probing direction, denoted \hat{Z}_i ($i=1,2,3$), was defined as the average of the impedance values of the matrix pixels in two opposite faces of normal n_i ($i=1,2,3$). The reproducibility of the assessment of \hat{Z} , obtained after imaging the face of the same bone four times on different days, was found to be 1.4%.

The 2D cross-sectional porosity was calculated from the segmented Z-maps in the 1–2 plane, i.e. perpendicular to the bone axis (Fig. 1), as the ratio of the pores area to the total bone surface. Porosity is usually assumed to vary only slightly across sample thickness. This assumption is reasonably met with the typical sample thickness of 7 mm, given that (1) the Haversian canals are roughly aligned with the bone axis and (2) the osteon length is 4 mm on average in human femoral mid-diaphysis [19]. However in our experience, large resorption cavities visible on a cross-sectional surface can introduce a significant bias in the estimation of volumetric porosity from surface porosity. To overcome this limitation, we estimated the volumetric porosity of each sample (denoted Por) as the average value of the cross-sectional porosities assessed on the two opposite faces in the 1–2 planes.

Synchrotron radiation microtomography (SR- μ CT)

To comfort our assumption that Por is a good surrogate for the volumetric porosity, a subset of specimens was imaged using 3D SR- μ CT. SR- μ CT measurements were performed on the imaging beamline ID19 at the ESRF (European Synchrotron Radiation Facility, Grenoble, France). The beam energy was tuned to 27 keV by using a (Si111) double crystal monochromator. A full set of 2D radiographic images was recorded using a CDD detector (FReLoN camera; ESRF Detector group) by rotating the sample in 1999 steps within a 360° range of rotation in about 35 min. We selected a pixel size of 5.4 μ m on the detector providing a 3D reconstructed image volume with a measured spatial resolution of about 10 μ m. Due to time limitations at the ESRF facilities, only ten of the twenty-one samples were imaged. After the 3D tomographic reconstruction and the conversion of the linear attenuation coefficients to degree of mineralization values expressed in g/cm³ of hydroxyapatite (HA) crystals [20], the 3D-porosity was derived from the segmented SR- μ CT images, following a fixed threshold set to 0.7 g HA/cm³.

Micromechanical model

Micromechanical models are useful as a means of testing how changes of the bone microscale properties affect its mesoscopic behavior. The modeled behavior depends in particular on hypothesized organizational patterns and elastic symmetry of the model material phases. In this work, a model of cortical bone mesoscopic elasticity based on asymptotic homogenization (AH) was used (source code available online [21]). This micromechanical method was chosen

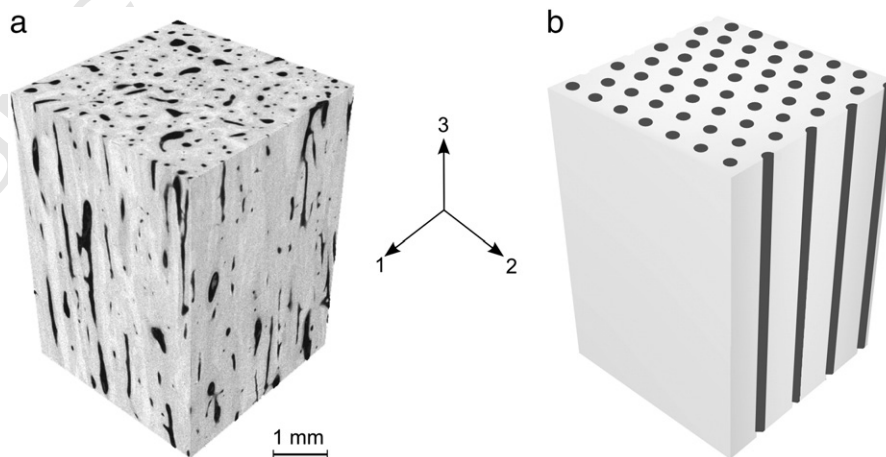


Fig. 1. (a) 3D reconstruction of a cortical bone volume from SR- μ CT data. The samples faces are oriented according to the radial (1), circumferential (2), and axial (3) axes defined by the anatomic shape of the femoral diaphysis. (b) Idealization of cortical bone as a homogeneous anisotropic matrix pervaded by infinite cylindrical pores, which are periodically distributed within the matrix material, specifically on a hexagonal lattice.

Table 1
Experimental data (mean \pm std [range]).

Mesoscopic elastic coefficients [GPa]					
C ₁₁	C ₂₂	C ₃₃	C ₄₄	C ₅₅	C ₆₆
19.3 ± 2.2 [15.6–23.2]	19.8 ± 2.2 [15.0–22.8]	29.2 ± 3.2 [23.3–34.5]	5.8 ± 0.8 [4.3–7.1]	5.6 ± 0.8 [3.8–6.8]	4.2 ± 0.6 [2.8–5.2]
Mean acoustic impedance of the bone matrix [MRayl]					
\hat{Z}_1		\hat{Z}_2	\hat{Z}_3		
7.4 ± 0.4 [6.4–8.2]		7.3 ± 0.3 [6.7–7.9]	8.7 ± 0.4 [8.1–9.6]		
Vascular porosity [%]					
13.5 ± 6.8 [2.9–26.9]					

for its stability, even at high porosities. The theory was described in details in the case of matrix isotropy in Parnell and Grimal [22]. The model hypothesizes that cortical bone can be regarded as a homogeneous transversely isotropic (TI) matrix pervaded by cylindrical pores, which are periodically distributed within the matrix material, specifically on a hexagonal lattice (Fig. 1). Here, the plane normal to the pores (1–2 plane) is the plane of isotropy for the matrix. The representation leads to transversely isotropic elasticity at the mesoscale (isotropy in the 1–2 plane), which is a reasonable approximation in human femoral mid-diaphysis [2,12]. Given an elastic tensor c^m describing the matrix elasticity, an elastic tensor c^p describing the elasticity of the material within the pores, and the volume fraction of pores, a homogenized elastic tensor C^* at the mesoscale is calculated. The elastic tensor of the bone matrix was identical for all samples. Its coefficients were determined by minimizing the L2-norm of the relative error between the experimental (C) and homogenized (C^*) mesoscopic elasticity values over the twenty-one samples. Hence c^m is the tensor which minimizes the objective function defined as:

$$H_0(c^m) = \sqrt{\sum_{k=1}^{21} \sum_{i=1}^6 \left(\frac{C_{ii;k} - C_{ii;k}^*(c^m, c^p, Por_k)}{C_{ii;k}} \right)^2} \quad (2)$$

where Por_k refers to the estimate of porosity of sample k assessed from impedance maps, and $C_{ii;k}$ and $C_{ii;k}^*$ to its experimental and homogenized elastic coefficients. Since the samples were kept moist during the measurements, the material in pores (undrained) was assumed to behave like bulk water, that is, bulk modulus and Poisson ratio were set to 2.3 GPa [23] and 0.4999 (quasi-incompressible), respectively, from which the terms of c^p can be calculated.

Statistics

The distribution normality and variance equality were confirmed using Shapiro–Wilk and Bartlett's tests respectively. One-way analysis of variance (ANOVA) followed by post-hoc comparisons using Tukey's HSD test were performed to evaluate the differences in the different directions for the longitudinal and shear elastic coefficients and for the mean acoustic impedance. Note that the influence of the anatomical quadrant on the elasticity was not investigated due to the small number of samples (posterior ($n=2$), lateral ($n=9$), and medial ($n=10$)). Adjusted R^2 (adj- R^2) from single linear and stepwise multiple regression analyses were used to characterize the relative contributions of the vascular porosity (Por) and bone matrix mean impedance in the different directions (\hat{Z}_i) to the mesoscopic elastic coefficients (C_{ii}). After the determination of the optimal matrix properties c^m in the AH model (Eq. (2)), the agreement between the experimental and homogenized elastic coefficients as obtained from the AH model was deduced from the linear regression parameters (adj- R^2 and root mean square error (RMSE)). All statistical results were considered significant for p-values less than 0.05. Statistics were made using the MatLab Statistics Toolbox (The Mathworks Inc., Natick, MA, USA) and JMP (SAS Institute Inc., Cary, NC).

Results

We evaluated the anisotropic elastic properties of the samples at two scales. At the mesoscale, ANOVA showed that the samples exhibited a strong elastic anisotropy which was reflected in the longitudinal elastic coefficients ($F=98$, $p<10^{-5}$) as well as in the shear elastic coefficients ($F=26$, $p<10^{-5}$). Precisely, we observed (Tukey HSD) $C_{33}>C_{11}$ (not different from C_{22}) and $C_{66}<C_{44}$ (not different from C_{55}). At the microscale, the bone matrix also exhibited anisotropy ($F=96$, $p<10^{-5}$), which was reflected in a significant higher impedance value along the bone axis compared to the two transverse directions \hat{Z}_1 and \hat{Z}_2 , which did not significantly differ. The average values of the mesoscopic elastic coefficients and the bone matrix mean impedance are summarized in Table 1. The p-values of the Tukey tests are given in Fig. 2.

The comparison, for a subset of ten samples, of the 3D-porosity obtained from the SR- μ CT to the estimated porosity value (Por) allowed to validate the assessment of volumetric porosity from the segmented impedance maps. Precisely, Por and the 3D-porosity were not significantly different (paired t -test, $p=0.48$) and were highly correlated as shown by the linear regression results (adj $R^2=0.98$, RMSE=0.94%, slope not significantly different from 1) (Fig. 3). Por was found to be (mean \pm sd) $13.5 \pm 6.8\%$, covering a wide range of values [3–27%].

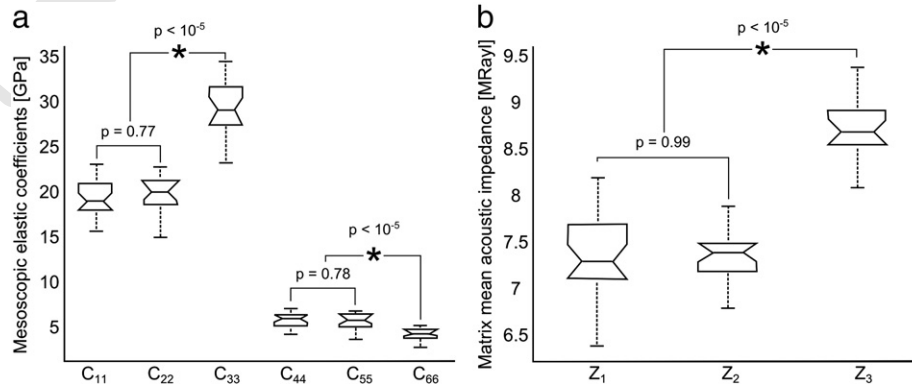


Fig. 2. Experimental results: (a) mesoscopic elastic coefficients (b) mean acoustic impedance of the bone matrix. On each box the central mark is the median, the edges are the 25th and 75th percentiles, the whiskers extend indicate the extreme values. The p-values from the post hoc multiple comparison Tukey's HSD tests are also given.

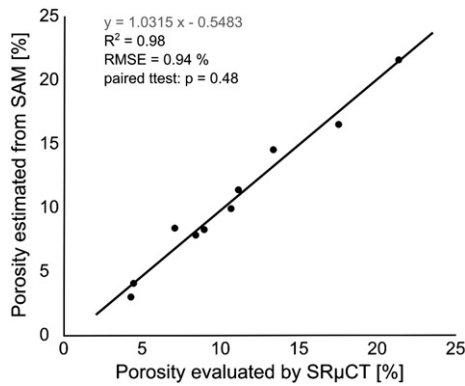


Fig. 3. Validation of the assessment of volumetric porosity from the segmented impedance maps on a subset of ten samples: the estimated value of the 'volumetric' porosity (Por) is plotted against the 3D-porosity obtained from SR- μ CT.

Table 2

Multivariate analysis regression (adjusted R^2 and RMSE): relative contributions of the vascular porosity (Por) and the matrix impedance (\hat{Z}_i) to the mesoscopic elastic coefficients (C_{ii}).

	Adjusted R^2 RMSE [GPa]	C_{11}	C_{22}	C_{33}	C_{44}	C_{55}	C_{66}
\hat{Z}_1		n.s.	n.s.	n.s.	n.s.	n.s.	n.s.
\hat{Z}_2		n.s.	n.s.	n.s.	n.s.	n.s.	n.s.
\hat{Z}_3		0.21*	n.s.	0.26*	0.22*	0.26*	0.16*
Por		0.79**	0.76**	0.74**	0.84**	0.72**	0.78**
$\hat{Z}_1, \hat{Z}_2, \hat{Z}_3$		1.01	1.09	1.64	0.31	0.44	0.30
$Por, \hat{Z}_1, \hat{Z}_2, \hat{Z}_3$		0.79**	0.76**	0.74**	0.84**	0.72**	0.78**
		1.01	1.09	1.64	0.31	0.44	0.30

n.s.: not significant ($p > 0.05$).

* $p < 0.05$.

** $p < 10^{-5}$.

A weak but significant correlation was found between all C_{ii} , except C_{22} , and \hat{Z}_3 (bone axis direction) ($\text{adj-}R^2 < 0.25$, $p = [0.01–0.04]$) (Table 2). No significant correlation was found between the C_{ii} and the matrix impedance in the radial and circumferential directions (\hat{Z}_1 and \hat{Z}_2). The mesoscopic elastic coefficients were well correlated to the porosity ($\text{adj-}R^2 = [0.72–0.84]$, $p < 10^{-5}$). The use of a stepwise regression analysis showed no improvement of the correlation when adding the bone matrix impedance (\hat{Z}_i) to the porosity to explain the mesoscopic elasticity variations between samples.

The transversely isotropic elastic tensor of the matrix (c^m) which allowed the best agreement (in the sense of Eq. (2)) between mea-

sured and modeled mesoscopic elastic properties was found to be $c_{11}^m = c_{22}^m = 26.8$ GPa, $c_{33}^m = 35.1$ GPa, $c_{44}^m = c_{55}^m = 7.3$ GPa, $c_{66}^m = 5.8$ GPa, $c_{13}^m = c_{23}^m = 15.3$ GPa, and thus $c_{12}^m = c_{11}^m - 2c_{66}^m = 15.2$ GPa.

The experimental mesoscopic elastic coefficients correlated well with the effective elastic coefficients as computed from the AH model ($\text{adj-}R^2 = [0.78–0.82]$, $p < 10^{-5}$) (Fig. 4). The precision of the model prediction was evaluated by means of the RMSE absolute and relative values: $C_{11} = 1.0$ GPa (5.2%), $C_{22} = 1.2$ GPa (6%), $C_{33} = 1.7$ GPa (5.6%), $C_{44} = 0.3$ GPa (5.5%), $C_{55} = 0.4$ GPa (8.5%), $C_{66} = 0.3$ GPa (7.6%).

Discussion

To our knowledge, the current work is the first to provide, for the same set of samples, measurements of the anisotropic elastic properties at two scales together with an evaluation of the cortical porosity. A set of human femoral cortical bone data, obtained on twenty-one samples from ten donors, was used to investigate the relative contributions of both the matrix elasticity and the porosity to the bone mesoscopic elasticity.

The experimental data corroborated well with previous studies, be it in respect of the mesoscopic elastic coefficients [2,3,12], the mean acoustic impedance of the bone matrix [14,17], or the range of the intracortical porosity [24–26].

Impedance measurements suggested that the average elastic properties of the mineralized matrix did not undergo large variations in the different samples (with coefficients of variation of the \hat{Z}_i all inferior to 6%). The limited variations of bone matrix elasticity reflected in Z might explain the lack of correlation between the mean acoustic impedance of the matrix and the mesoscopic elastic coefficients. A literature review reveals that such modest variations of the bone matrix properties have been observed in a number of studies. Cross-sectional reports have shown that the mean degree of mineralization of bone does not exhibit large variations between individuals, independently of age [10,27,28] and gender [27]. A few studies have measured the matrix elasticity on several individuals at the same cortical bone site (femoral diaphysis and neck [29], femoral diaphysis [7], radius [14]). Similarly, they all reported small changes in the mean value of the matrix elasticity (average of several measurements points on a surface of at least 1 mm) with coefficients of variation ranging between 3 and 10%. Hence, although the bone matrix elasticity is known to display strong local heterogeneities (in particular between the osteonal and interstitial tissues), its mean value over a few millimeters remains relatively constant in healthy individuals. However, a selection of bone specimens in a population with known bone pathologies could result in a wider variation of matrix material properties and lead to different conclusions.

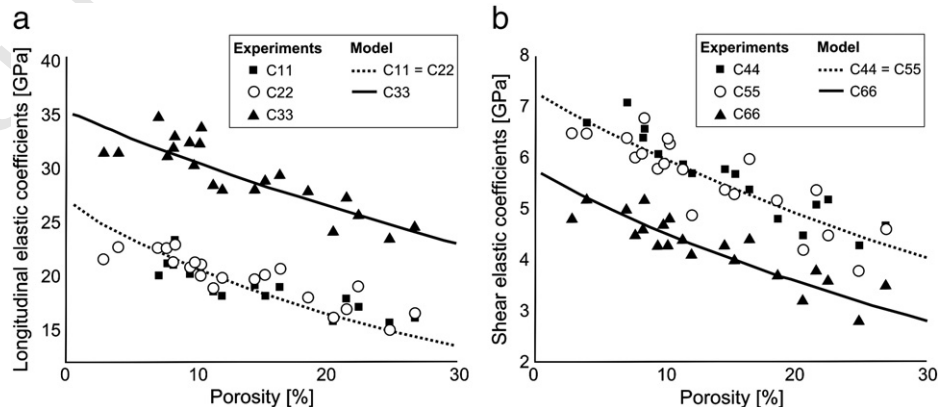


Fig. 4. (a) Longitudinal and (b) shear mesoscopic elastic coefficients versus porosity: results from experiments (■, ○, ▲) and asymptotic homogenization model (solid and dotted lines). Note that all the homogenized elastic coefficients computed from the AH model are obtained using a unique set of elastic constants for the bone matrix.

Our results demonstrate that, for an elderly population, the change in porosity is the major determinant of the variations of the anisotropic elastic coefficients at the mesoscale, at least in the femoral mid-diaphysis. To our knowledge, only one study has experimentally examined the impact of porosity variations on the elasticity of human femoral cortical bone in several directions [8]. While they also found a strong dependence of the Young's moduli and shear moduli on porosity ($R^2 = [0.66–0.72]$), they observed no significant correlation between the elastic properties in the transverse direction and the porosity, in contrast to our findings.

The fact that all the mesoscopic elastic coefficients have a dependency on the porosity is supported by the theoretical results obtained with several models using different homogenization approaches [1,30–34]. We compare the outcome of a homogenization model to experimental data for known values of porosities associated to a number of bone material volumes. As far as we know, only two previous studies confronted experimental results with the predictions of a micromechanical model. However, the elastic constants were not assessed on the same specimens [31], or the shear constants were lacking [35]. In our study, because six elastic coefficients have been measured for each sample, a large data set is available for the comparison. We found that modeling cortical bone as a two-phase composite with a transversely isotropic matrix pervaded by cylindrical pores provided a good estimate of the elasticity variations at the mesoscale, as shown by the strong correlations (relative RMSE = $[5.2–8.5\%]$) between the experimental results and the prediction of the micromechanical model. Note, however, that the homogenized elasticity C^* is not strictly independent of the mesoscale experimental data C because the matrix elasticity of the model (c^m) was determined such that the agreement between C and C^* is optimum (Eq. (2)).

It is noteworthy that the model was particularly efficient considering its ability to fit all experimental mesoscopic elastic coefficients with a relatively good accuracy using a unique elastic tensor for the matrix and the pores and a sample-dependent porosity. This was despite the many idealizations of the model, in particular the elastic properties of the matrix and the modeling of the pores. Universal, homogeneous, elastic properties were assigned to the bone matrix. The choice of a unique matrix was supported by the small change in the average elastic properties of the matrix, as testified by the matrix impedance data. We verified that the optimized set of TI elastic properties assigned to the bone matrix (c^m) were physically acceptable. In fact, once converted into engineering moduli ($E_T = 16.5$ GPa, $E_L = 24.0$ GPa, $G_T = 5.8$ GPa, $G_L = 7.3$ GPa), the matrix elastic properties were found consistent with the nanoindentation values in human femoral bone available in literature [36–38]. Moreover, the matrix elastic coefficients (c^m) used in our model compared well with those derived from the experimental acoustic impedance mean values using the conversion relationship between Z and c^m [15]. Precisely, the elastic coefficients of the matrix as derived from the Z_i ($i = 1, 2, 3$) ($c_{11}^m \text{exp} = 28.7 \pm 3.1$ GPa, $c_{22}^m \text{exp} = 28.5 \pm 2.3$ GPa and $c_{33}^m \text{exp} = 40.7 \pm 3.3$ GPa) were in agreement with the elastic coefficients assigned in the model ($c_{11}^m = c_{22}^m = 26.8$ GPa, $c_{33}^m = 35.1$ GPa). The vascular porosity was idealized as infinite cylinders of circular cross-section aligned along the bone long axis. Hence, the pores were modeled as continuous even though a discontinuous representation might seem more realistic. However, we have found that, for aspect ratios (length of the pore/diameter of the pore) larger than 5, modeling the pores as infinite cylinders yields a very good approximation (less than 1% error) of discontinuous pores with typical aspect ratio of the Haversian canal [39]. Although this representation has been commonly used for modeling cortical bone [30,31,35], it does not take into account the variability of pores shapes, size, and distribution. Considering the gradient of porosity from the endosteal to the periosteal region [14,24] or the change in the pores size [26,32] may improve the predictions of the bone effective elastic properties.

The remaining part of experimentally determined elasticity C which is not explained by the model is due to experimental uncertainties and model assumptions. The latter comprise the assumptions regarding the pores as mentioned above and the fact that some variability of the matrix properties exists between different samples.

A first limitation of the study arises from the estimation of the sample porosity as the average value of the cross-sectional porosities assessed on the two opposite transverse faces. However, the validation of the porosity evaluation with 2D SAM on ten samples against the vascular porosity as obtained from 3D SRμCT data confirmed that Por is a good proxy for the vascular porosity. A second limitation in the study is the fact that all donors were elderly female donors (with a mean age superior to 80 years). Although the bone matrix elasticity has been shown to be independent from age and gender [40], aging strongly affects the range of porosity and could change the relative contributions of the matrix elasticity and the porosity to the mesoscopic elasticity in younger individuals. Thus the conclusions of this study hold true only for an aged population, which is most commonly affected by osteoporosis and bone fragility. Finally, in spite of a limited sample size ($n = 21$ from 10 subjects), the range of values covered by the porosity (from 3 to 27%) was wide enough to provide conclusive results.

In summary, the findings of this paper demonstrate that, in aged women, the changes in porosity prevail over those of matrix elasticity to drive the variations of the bone mesoscopic elasticity. The impact of the porosity on the elasticity is all the more important considering the increased intracortical porosity as a consequence of aging [10,26,41–43] and disease, e.g. hyperparathyroidism, osteoporosis [44]. In particular, Zebaze et al. [43] showed that 84% of the bone loss occurs after the age of 65 of which 68% would be cortical bone manifested as an increase of cortical porosity. Moreover, the increase of cortical porosity, pointed out as the dominant factor occurring in elderly individuals, is known to reduce bone strength [45]. A simple mechanical model was proposed to interpret the experimental data: the dependence on porosity of shear and longitudinal elastic properties in the radial, circumferential, and axial directions of bone is correctly described when idealizing bone as a two-phase material with a 'universal' (same for all bone samples) transversely isotropic matrix pervaded by cylindrical pores.

Acknowledgments

This work has been conducted within the European Associated Laboratory "Ultrasound Based Assessment of Bone" (ULAB) and was supported by the ESRF Long Term Proposal MD431.

References

- Grimal Q, Raum K, Gerisch A, Laugier P. A determination of the minimum sizes of representative volume elements for the prediction of cortical bone elastic properties. *Biomech Model Mechanobiol* 2011, doi:10.1007/s10237-010-0284-9.
- Espinoza Orias AA, Deuerling JM, Landrigan MD, Renaud JE, Roeder RK. Anatomic variation in the elastic anisotropy of cortical bone tissue in the human femur. *J Mech Behav Biomed Mater* 2009;2:255–63.
- Ashman RB, Cowin SC, Van Buskirk WC, Rice JC. A continuous wave technique for the measurement of the elastic properties of cortical bone. *J Biomech* 1984;17:349–61.
- Rudy DJ, Deuerling JM, Espinoza Orias AA, Roeder RK. Anatomic variation in the elastic inhomogeneity and anisotropy of human femoral cortical bone tissue is consistent across multiple donors. *J Biomech* 2011, doi:10.1016/j.jbiomech.2011.04.009.
- Cowin SC. Bone poroelasticity. *J Biomech* 1999;32:217–38.
- Wachter NJ, Krischak GD, Mentzel M, Sarkar MR, Ebinger T, Kinzel L, et al. Correlation of bone mineral density with strength and microstructural parameters of cortical bone in vitro. *Bone* 2002;31:90–5.
- Rho JY, Zioupos P, Currey JD, Pharr GM. Microstructural elasticity and regional heterogeneity in human femoral bone of various ages examined by nanoindentation. *J Biomech* 2002;35:189–98.
- Dong XN, Guo XE. The dependence of transversely isotropic elasticity of human femoral cortical bone on porosity. *J Biomech* 2004;37:1281–7.
- Currey JD. The effect of porosity and mineral content on the Young's modulus of elasticity of compact bone. *J Biomech* 1988;21:131–9.

- [10] McCalden RW, McGeough JA, Barker MB, Court-Brown CM. Age related changes in the tensile properties of cortical bone. *J Bone Joint Surg Am* 1993;75: 1193–205.
- [11] Currey JD, Zioupos P. The effect of porous microstructure on the anisotropy of bone-like tissue: a counterexample. *J Biomech* 2001;34:707–8.
- [12] Yoon HS, Katz JL. Ultrasonic wave propagation in human cortical bone – II. Measurements of elastic properties and microhardness. *J Biomech* 1976;9: 459–64.
- [13] Raum K, Leguerney I, Chandelier F, Bossy E, Talmant M, Saïed A, et al. Bone microstructure and elastic tissue properties are reflected in QUS axial transmission measurements. *Ultrasound Med Biol* 2005;31:1225–35.
- [14] Saïed A, Raum K, Leguerney I, Laugier P. Spatial distribution of anisotropic acoustic impedance assessed by time-resolved 50-MHz scanning acoustic microscopy and its relation to porosity in human cortical bone. *Bone* 2008;43:187–94.
- [15] Preininger B, Checa S, Molnar FL, Fratzi P, Duda GN, Raum K. Spatial-temporal mapping of bone structural and elastic properties in a sheep model following osteotomy. *Ultrasound Med Biol* 2011;37:474–83.
- [16] Hofmann T, Heyroth F, Meinhard H, Franzel W, Raum K. Assessment of composition and anisotropic elastic properties of secondary osteon lamellae. *J Biomech* 2006;39: 2282–94.
- [17] Rupin F, Saïed A, Dalmas D, Peyrin F, Hauptert S, Raum K, et al. Assessment of Microelastic Properties of Bone Using Scanning Acoustic Microscopy: A Face-to-face Comparison with Nanoindentation. *Jpn J Appl Phys* 2009;48:07GK01.
- [18] Raum K, Leguerney I, Chandelier F, Talmant M, Saïed A, Peyrin F, et al. Site-matched assessment of structural and tissue properties of cortical bone using scanning acoustic microscopy and synchrotron radiation μ CT. *Phys Med Biol* 2006;51:733–46.
- [19] Cooper DML, Thomas CDL, Clement JG, Hallgrímsson B. Three-dimensional microcomputed tomography imaging of basic multicellular unit-related resorption spaces in human cortical bone. *Anat Rec A* 2006;228A:806–16.
- [20] Nuzzo S, Peyrin F, Cloetens P, Baruchel J, Boivin G. Quantification of the degree of mineralization of bone in three dimensions using synchrotron radiation microtomography. *Med Phys* 2002;29:2672–81.
- [21] Grimal Q, Parnell WJ. Cortical bone homogenization. Retrieved January 15, 2011 from <http://www.labos.upmc.fr/lip/spip.php?rubrique133>.
- [22] Parnell WJ, Grimal Q. The influence of mesoscale porosity on cortical bone anisotropy. Investigations via asymptotic homogenization. *J R Soc Interface* 2009;6:97–109.
- [23] Anderson CB. Mechanics of fluids. In: Baumeister T, editor. *Mark's saturated handbook for mechanical engineers*. New York: MacGraw-Hill; 1967. p. 3.48–76.
- [24] Bousson V, Bergot C, Meunier A, Barbot F, Parlier-Cuau C, Laval-Lantet AM, et al. CT of the middiaphyseal femur: cortical bone mineral density and relation to porosity. *Radiology* 2000;217:179–87.
- [25] Thomas CDL, Feik SA, Clement JG. Regional variation of intracortical porosity in the midshaft of the human femur: age and sex differences. *J Anat* 2005;206: 115–25.
- [26] Cooper DML, Thomas CDL, Clement JG, Turinsky AL, Sensen CW, Hallgrímsson B. Age-dependent change in the 3D structure of cortical porosity at the human femoral midshaft. *Bone* 2007;40:957–65.
- [27] Boivin G, Meunier PJ. The degree of mineralization of bone tissue measured by computerized quantitative contact microradiography. *Calcif Tissue Int* 2002;70: 503–11.
- [28] Bergot C, Wu Y, Jolivet E, Zhou LQ, Laredo JD, Bousson V. The degree of mineralization in the human femoral shaft change with age and sex in a microradiographic study. *Bone* 2009;45:435–42.
- [29] Hoffer CE, Moore KE, Kozloff K, Zysset PK, Brown MB, Goldstein SA. Heterogeneity of bone lamellar-level elastic moduli. *Bone* 2000;26:603–9.
- [30] Hellmich C, Ulm FJ, Dormieux L. Can the diverse elastic properties of trabecular and cortical bone be attributed to only a few tissue-independent phase properties and their interactions? *Biomech Model Mechanobiol* 2004;2:219–38.
- [31] Dong XN, Guo XE. Prediction of cortical bone elastic constants by a two-level micromechanical model using a generalized self-consistent method. *J Biomed Eng* 2006;128:309–16.
- [32] Baron C, Talmant M, Laugier P. Effect of porosity on effective diagonal stiffness coefficients (c_{ii}) and elastic anisotropy of cortical bone at 1 MHz: a finite-difference time domain study. *J Acoust Soc Am* 2007;122:1810–7.
- [33] Grimal Q, Raum K, Gerisch A, Laugier P. Derivation of the mesoscopic elasticity tensor of cortical bone from quantitative impedance images at the micron scale. *Comput Meth Biomech Biomed Eng* 2008;11:147–57.
- [34] Grimal Q, Rus G, Parnell WJ, Laugier P. A two-parameter model of the effective elastic tensor for cortical bone. *J Biomech* 2011;44:1621–5.
- [35] Deuerling JM, Weimin Y, Espinoza Orias AA, Roeder RK. Specimen-specific multiscale model for the anisotropic elastic constants of human cortical bone. *J Biomech* 2009;42:2061–7.
- [36] Rho JY, Roy II ME, Tsui TY, Pharr GM. Elastic properties of microstructural components of human bone tissue as measured by nanoindentation. *J Biomed Mater Res A* 1999;45:48–54.
- [37] Turner CH, Rho JY, Takano Y, Tsui TY, Pharr GM. The elastic properties of trabecular and cortical bone tissues are similar: results from two microscopic measurements techniques. *J Biomech* 1999;32:437–41.
- [38] Franzoso G, Zysset PK. Elastic anisotropy of human cortical bone secondary osteons measured by nanoindentation. *J Biomech Eng* 2009;131:021001-1.
- [39] Granke M, Grimal Q, Parnell WJ, Saïed A, Peyrin F, Laugier P. Elasticity and porosity in human cortical bone: models and experiments. In *Congrès Français de Mécanique*, Besançon; 2011.
- [40] Hoffer CE, Moore KE, Kozloff K, Zysset PK, Goldstein SA. Age, gender, and bone lamellae elastic moduli. *J Orthop Res* 2000;18:432–7.
- [41] Bousson V, Meunier A, Bergot C, Vicaud E, Rocha MA, Morais MH, et al. Distribution of intracortical porosity in human midfemoral cortex by age and gender. *J Bone Miner Res* 2001;16:1308–17.
- [42] Burghardt AJ, Kazakia GJ, Ramachandran S, Link TM, Majumdar S. Age- and gender-related differences in the geometric properties and biomechanical significance of intracortical porosity in the distal radius and tibia. *J Bone Miner Res* 2010;25:983–93.
- [43] Zebaze R, Ghasem-Zadeh A, Bohte A, Iuliano-Burns S, Mirams M, Ian Price R, et al. Intracortical remodeling and porosity in the distal radius and post-mortem femurs of women: a cross-sectional study. *Lancet* 2010;375:1729–36.
- [44] Chavassieux P, Seeman E, Delmas PD. Insights into material and structural basis of bone fragility from diseases associated with fractures: how determinants of the biomechanical properties of bone are compromised by disease. *Endocr Rev* 2007;28:151–64.
- [45] Yeni YN, Brown CU, Wang Z, Norman TL. The influence of bone morphology on fracture toughness of the human femur and tibia. *Bone* 1997;21:453–9.